



ISTITUTO NAZIONALE DI RICERCA METROLOGICA Repository Istituzionale

Density and derived properties of standard seawater up to high pressure in stable and metastable states

This is the author's submitted version of the contribution published as:

Original

Density and derived properties of standard seawater up to high pressure in stable and metastable states / Romeo, R.; Giuliano Albo, P. A.; Lago, S.. - In: DEEP-SEA RESEARCH PART I-OCEANOGRAPHIC RESEARCH PAPERS. - ISSN 0967-0637. - 177:(2021), p. 103624. [10.1016/j.dsr.2021.103624]

Availability:

This version is available at: 11696/72936 since: 2022-02-11T16:12:32Z

Publisher:

ELSEVIER SCIENCE LTD

Published

DOI:10.1016/j.dsr.2021.103624

Terms of use:

This article is made available under terms and conditions as specified in the corresponding bibliographic description in the repository

Publisher copyright

(Article begins on next page)

1 Thermal properties of standard seawater up to high pressure
2 in stable and metastable states

3 R. Romeo^{a,*}, P.A. Giuliano Albo^a, S. Lago^a

4 ^a*Istituto Nazionale di Ricerca Metrologica, Strada delle Cacce 91, Turin 10135, Italy*

5 **Abstract**

6 In this work, a consolidated experimental apparatus for measuring the density of
7 liquids, such as high pressure and metastable states, based on the isochoric method,
8 was exploited to measure thermal properties of seawater. Density of standard seawater
9 was measured in a wide range of temperature and pressure, specifically from (261.15 to
10 313.15) K and up to 110 MPa. All terms contributing to the uncertainty in determining
11 the volume and the mass of the specimen were evaluated, obtaining a relative expanded
12 uncertainty of seawater density around 0.05 % ($k = 2$). Experimental results were
13 fitted by using a 8-parameters function of specific volume as a function of temperature
14 and pressure. Using the obtained expression, density, isobaric thermal expansion, and
15 isothermal compressibility of seawater were calculated from (263.15 to 313.15) K and
16 for pressures between (1 and 105) MPa. A comparison with the predictions obtained
17 by the Thermodynamic Equation of Seawater - 2010 (TEOS-10) shows a general good
18 agreement that worsens when metastable states are considered.

19 *Keywords:* seawater, density, pycnometer, metastable states, thermal properties

20 **1. Introduction**

21 Seawater is not only the environment where more than 200 thousands documented
22 species live, but it is also the reservoir of the thermal energy of our planet. The dis-
23 tribution of the energy content is driven by geographical variations of the temperature,
24 the pressure and the density that are at the origin of small and large scale circulations
25 (Wright et al., 2011). Furthermore, the energy exchanges between seawater and the at-
26 mosphere significantly contribute to the formation and to the evolution of ordinary and
27 extraordinary climate events. To monitor and provide predictive models for forecast and
28 climate change, accurate measurements of physical and chemical properties of seawater
29 are strongly demanded. Beside the role played to sustain the Earth's ecosystem and
30 climate, seawater is also exploited as cooling fluid in power stations, as heating fluid
31 for the regasification of liquefied natural gas (LNG) and as feed stock to produce fresh
32 water by desalination processes. For all the applications, it is necessary to have accurate
33 predictions for the density of the fluid, at high pressure and at different temperatures, to
34 optimize the production of the industrial plants (Safarov et al., 2009, 2013).

*Corresponding author

Email address: r.romeo@inrim.it (R. Romeo)

35 The density of seawater changes as a function of the depth below sea surface. Specif-
36 ically, the pressure range in oceanic seawater is from 0.1 MPa at the sea surface to ap-
37 proximately 108.6 MPa at the deepest level. The ocean temperature ranges, on average,
38 approximately from (273.15 to 313.15) K. In addition to density, derived properties are
39 useful to understand real ocean processes. For example, thermal expansivity is needed to
40 figure out great gradients due to hot (close to critical temperature) seawater vents from
41 ocean floor (Safarov et al., 2012).

42 Seawater freezing point is around 271 K; however, it can be cooled to lower tem-
43 peratures without crystallization (supercooled seawater). This phenomenon is observed
44 both in Antarctic and Arctic oceans, occurring as a consequence of the melting of ice
45 shelves at depth (ice shelves cavity) and the formation of sea ice at the surface. As
46 shown in Haumann et al. (2020), the deep vertical extent of the supercooled seawater
47 column can be important for both vertical heat transport and for the vertical transport of
48 salt, carbon, oxygen, and nutrients. Furthermore, supercooled seawater is the basis for
49 the creation of the "platelet ice", which forms by nucleation in supercooled layers of sea-
50 water near ice shelves, both in Antarctica and Arctic, under particular conditions able to
51 generate and maintain supercooling (Hoppmann et al., 2020). Platelet ice involves both
52 physical processes and biogeochemical cycles, hosting the associated peculiar ecosys-
53 tem (Katlein et al., 2020).

54 The thermodynamic modelling of seawater poses many problems since the system is
55 composed by a large number of different dissolved salts in small quantities, but strongly
56 interacting. For this reason, a complete description of the interactions as a function of
57 the composition has been avoided in favor of the adoption of salinity as a new indepen-
58 dent variable, defined on the basis of chemical properties. Although the introduction
59 of salinity allowed to solve practical problems, the chosen definition is not unique and
60 still debated, as claimed by Seitz et al. (2011) and Feistel (2018).

61 Since 2010, the thermodynamic of seawater is described by the Thermodynamic
62 Equation of Seawater - 2010, or TEOS-10 (IOC et al., 2010), in terms of absolute salin-
63 ity, S_A , defined as the mass fraction of dissolved material per kilogram of seawater.
64 However, the validity of TEOS-10 and the experimental values in the literature do not
65 include the liquid metastable region.

66 Considering these aspects, in the present work standard seawater density is mea-
67 sured and modeled in a wide range of temperature and pressure. The pseudo-isochoric
68 method (pycnometry) was exploited to carry out density measurements up to 110 MPa,
69 to cover the whole natural range of ocean pressure, and for temperatures down to 261 K,
70 to investigate (even partially) supercooled seawater. These measurements were used
71 to implement a function of density able to operate in the entire range of temperature
72 and pressure here investigated, and to be used to derive the thermal properties, such as
73 isothermal compressibility and isobaric thermal expansivity.

74 **2. Materials and method**

75 To measure the density of seawater, and with the aim of carrying out measurements
76 even in metastable conditions, the isochoric method was exploited. As for the previ-
77 ous work Romeo et al. (2018), the method was chosen because of its versatility and

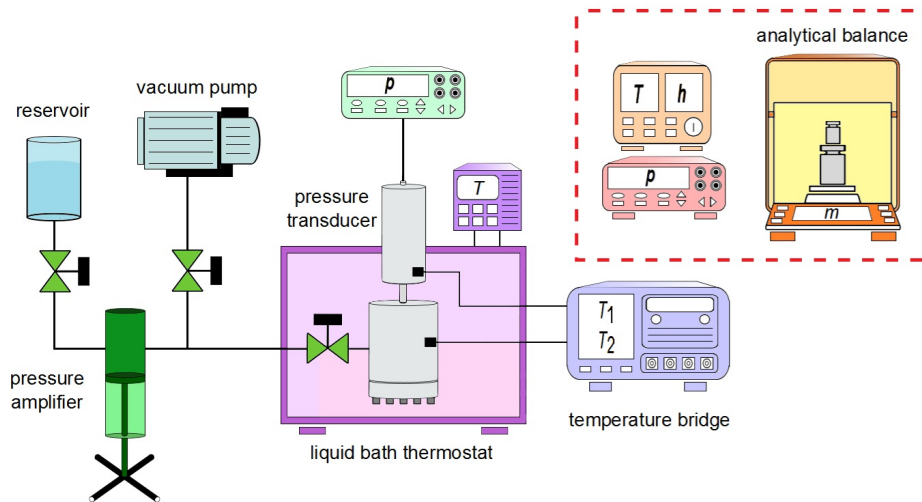


Figure 1: Schematic representation of the experimental apparatus for carrying out density measurements of standard seawater.

78 capability to operate in hard working conditions without being affected by the physical
 79 properties of the fluid (Goodwin et al., 2003).

80 This technique basically consists in measuring the mass and the volume of the mea-
 81 suring pycnometric cell. The main element of the experimental apparatus, the pyc-
 82 nometer, was designed and realized at Istituto Nazionale di Ricerca Metrologica and
 83 used in Romeo et al. (2018), where details on the pycnometer construction features and
 84 on the experimental setup can be found. The pycnometer was pressurized several times
 85 to test the sealing and the pressure stabilization was obtained up to 120 MPa.

86 The experimental apparatus schematically represented in Fig. 1 was arranged to
 87 control both temperature and pressure. A liquid bath thermostat (with a stabilization of
 88 ± 0.01 K), where the pycnometer is placed, is used to control the temperature, which is
 89 measured by two platinum resistance thermometers (PT100). The latter are sited one on
 90 the pycnometer main body and the other one on the pressure transducer. The thermome-
 91 ters are connected in 4-wire configuration to an industrial thermometer bridge. While
 92 the pycnometer is connected to a capacitance high pressure transducer with a full-scale
 93 range of 200 MPa for the pressure measurements. A high-pressure circuit consisting of
 94 a pressure amplifier and a system of valves are arranged to connect to the tank at am-
 95 bient conditions, fill the pycnometer, and increase the pressure inside. To complete the
 96 measurement, an analytical balance with a resolution of 0.1 mg, stainless steel standard
 97 weights to measure the mass, and sensors to monitor ambient temperature, pressure and
 98 relative humidity to calculate air density, is used.

99 To start the measuring procedure, the pycnometer is filled to a certain pressure using
 100 the pressure amplifier and the high pressure circuit. Then, it is placed into the thermo-
 101 static liquid bath. The temperature is slowly decreased, so that the sample reaches the
 102 metastable liquid condition avoiding crystallization. To this scope, it is required from

103 1 hour up to 3 hours (at the lower temperatures) to change the temperature by 1 K be-
 104 low the triple point. The temperature and the pressure are recorded at the equilibrium:
 105 when temperature and pressure stabilization is within 0.01 K and 0.2 MPa, respectively
 106 (usually around one hour is required). At the end of the cycle, the pycnometer is taken
 107 off the thermostat and carefully cleaned and dried from the thermostatic liquid (ethanol)
 108 before the weighing for the mass determination.

109 Once the measurements were complete, the density of seawater sample was mea-
 110 sured by a commercial vibrating tube densimeter at atmospheric pressure, with an un-
 111 certainty of 30 ppm as estimated by Romeo et al. (2019), to verify the composition had
 112 not changed.

113 2.1. Determination of the mass

114 The mass of seawater was determined by means of the gravimetric method. Weigh-
 115 ing was performed using a commercial analytical balance employed as a comparator
 116 with stainless steel standard masses (Davidson et al., 2004), by the double substitution
 117 method (OIML R111-1, 2004). Therefore, the mass M was obtained by the value of
 118 the certified standard weights, M_{eq} , and the difference of the readings, ΔR :

$$M = M_{\text{eq}} + \Delta R . \quad (1)$$

119 Seawater mass, m , was obtained by the difference between the mass of the pycnome-
 120 ter filled with the seawater sample, M_{ssw} , and the mass of the empty pycnometer, M_0 ,
 121 corrected for the buoyancy, by the following relation

$$m = M_{\text{ssw}} \left(1 - \frac{\rho_{\text{air}}}{\rho_{\text{std}}} \right) - M_0 \left(1 - \frac{\rho_{\text{air}}}{\rho_{\text{std}}} \right) , \quad (2)$$

122 where ρ_{air} is the density of air during the weighing, and $\rho_{\text{std}} = 8 \text{ g} \cdot \text{cm}^{-3}$ is the standard
 123 weights density.

124 2.2. Determination of the volume

125 The gravimetric method was also adopted to measure the volume of the pycnometer
 126 (Lorefice et al., 2014). Thus, the pycnometer was weighted both empty and filled with
 127 ordinary bi-distilled water (used as reference fluid) at the temperature T_0 and pressure
 128 p_0 , corresponding to a thermodynamic state of water density known with low uncer-
 129 tainty (0.003 % for the thermodynamic state here investigated). Water density is pro-
 130 vided by the equation of state of the International Association for Properties of Water
 131 and Steam, i.e., IAPWS-95 formulation by Wagner and Pruss (2002).

132 The pycnometer mass (empty and filled with water) was measured by comparison
 133 with standard weights by the double substitution method, using the analytical balance as
 134 comparator. During the weighing, atmospheric parameters were monitored to correct
 135 for the buoyancy in air. So that, the reference volume was determined as

$$V_0 (T_0, p_0) = \frac{M_{\text{ref}} - M_0}{\rho_{\text{ref}} (T_0, p_0) - \rho_{\text{air}}} \left(1 - \frac{\rho_{\text{air}}}{\rho_{\text{std}}} \right) , \quad (3)$$

136 where M_{ref} is the mass of the pycnometer filled with ordinary water, M_0 is the mass
 137 of the empty pycnometer, ρ_{ref} is the reference water density, ρ_{air} is the air density, and
 138 $\rho_{\text{std}} = 8 \text{ g} \cdot \text{cm}^{-3}$ is the standard weights density. The reference volume of the pycnome-
 139 ter at $T_0 = (293.21 \pm 0.01) \text{ K}$ and $p_0 = (50.8 \pm 0.2) \text{ MPa}$ is $V_0 = (11.655 \pm 0.002) \text{ cm}^3$.

140 To account for the variation of the volume as a function of temperature, T , and
 141 pressure, p , the value of V_0 was corrected by the thermal expansion coefficient and the
 142 compressibility coefficient, as follows

$$V(T, p) = V_0(T_0, p_0)[1 + \alpha(T - T_0) + \beta(p - p_0)], \quad (4)$$

143 where α and β are the thermal expansion and the isothermal compressibility of the
 144 pycnometer, respectively.

145 The values of α and β were determined experimentally, by performing measuring
 146 cycles with a reference fluid, i.e., ordinary water. Measurements were carried out using
 147 bi-distilled water, between (275 and 313) K and from (50 to 100) MPa. Considering the
 148 change of volume of Eq. 4, a function derived from the definition of density was used
 149 (see Romeo et al. (2018) for details). By fitting this linear function of both temperature
 150 and pressure, considering the literature density values of the IAPWS-95 formulation for
 151 each measurement, the α and β were obtained:

$$\alpha = (2.2 \pm 0.2) \cdot 10^{-5} \text{ K}^{-1}$$

$$\beta = (7.5 \pm 0.2) \cdot 10^{-5} \text{ MPa}^{-1}.$$

152 For the studied temperature and pressure range, variations of the elastic properties
 153 with temperature and pressure were within the declared uncertainty. For this reason,
 154 they are considered constant over the whole examined $T - p$ range.

155 3. Uncertainty analysis

156 3.1. Contribution of mass measurement

157 For the uncertainty analysis, according to Eq. 2, the mass of seawater is a function
 158 of all the quantities involved in the weighing procedure:

$$m = m(\Delta R, d, M_{\text{eq}}, \rho_{\text{air}}, \rho_{\text{std}}).$$

159 Therefore, the relative uncertainty in the estimation of seawater mass, $u(m)/m$, was
 160 calculated with the uncertainty propagation formula by

$$\frac{u(m)}{m} = \frac{1}{m} \left[\sigma^2(\Delta R) + \left(\frac{d}{\sqrt{6}} \right)^2 + u^2(M_{\text{eq}}) + \left(\frac{\partial m}{\partial \rho_{\text{air}}} \right)^2 u^2(\rho_{\text{air}}) + \left(\frac{\partial m}{\partial \rho_{\text{std}}} \right)^2 u^2(\rho_{\text{std}}) \right]^{\frac{1}{2}}, \quad (5)$$

161 where $\sigma(\Delta R)$ is the standard deviation of the the difference of readings, d is the digital
 162 resolution of the analytical balance as a triangular distribution (BIPM et al., 2008),

163 $u(M_{\text{eq}})$ is the uncertainty of the standard weights, provided by the calibration certificate.
 164 The uncertainties of the standard weights density, $u(\rho_{\text{std}})$, and air density, $u(\rho_{\text{air}})$, were
 165 negligible in the overall uncertainty. The sources of uncertainty affecting the mass
 166 measurement and associated relative magnitudes are listed in Table 1. The relative
 167 uncertainty of seawater mass is estimated to be 0.015%.

168 3.2. Contribution of the reference volume

169 According to Eq. 3, the uncertainty of the pycnometer reference volume, V_0 , was
 170 obtained taking into account the contributions of the mass of the reference fluid ($\Delta M =$
 171 $M_{\text{ref}} - M_0$), the densities of the reference fluid, air of laboratory and standard weights,
 172 and the filling temperature and pressure:

$$V_0 = V_0(\Delta M, \rho_{\text{ref}}, \rho_{\text{air}}, \rho_{\text{std}}, T_0, p_0) . \quad (6)$$

173 Applying the uncertainty propagation to Eq. 3, the relative uncertainty, $u(V_0)/V_0$, is
 174 assessed by

$$\frac{u(V_0)}{V_0} = \frac{1}{V_0} \left[\left(\frac{\partial V_0}{\partial \Delta M} \right)^2 u^2(\Delta M) + \left(\frac{\partial V_0}{\partial \rho_{\text{ref}}} \right)^2 u^2(\rho_{\text{ref}}) + \left(\frac{\partial V_0}{\partial \rho_{\text{air}}} \right)^2 u^2(\rho_{\text{air}}) + \right. \\ \left. \left(\frac{\partial V_0}{\partial \rho_{\text{std}}} \right)^2 u^2(\rho_{\text{std}}) + \left(\frac{\partial V_0}{\partial T_0} \right)^2 u^2(T_0) + \left(\frac{\partial V_0}{\partial p_0} \right)^2 u^2(p_0) \right]^{\frac{1}{2}} . \quad (7)$$

175 The uncertainty of the reference fluid mass, $u(\Delta M) = 0.002$ g, is given by the sum
 176 of the squares of the standard deviation of the readings difference, the balance reso-
 177 lution, and the standard weights uncertainty. As for the mass, the contributions of the
 178 uncertainties of the standard weights density, $u(\rho_{\text{std}})$, and the air density, $u(\rho_{\text{air}})$, resulted
 179 negligible in the overall uncertainty. As stated in Wagner and Pruss (2002), the uncer-
 180 tainty of IAPWS-95 for water density at 293.21 K and 50.8 MPa is $u(\rho_{\text{ref}}) = 0.003$ %.
 181 The uncertainty $u(T_0)$ of the temperature measurement is due to the calibration fit, the
 182 resolution of the instrument and the reading repeatability, and its value is within 0.01 K.
 183 The uncertainty of the pressure measurements $u(p_0)$ is due to the pressure transducer
 184 used and the measurement repeatability and it is 0.2 MPa.

185 The uncertainty of the pycnometer reference volume V_0 is lower than 0.01%; all
 186 the contributions considered and the associated relative magnitude are summarized in
 187 Table 1.

188 3.3. Volume uncertainty analysis

189 According to Eq. 4, the uncertainty of the pycnometer volume was determined con-
 190 sidering the volume V as a function of the reference volume V_0 , the thermal expansion
 191 coefficient α , the isothermal compressibility coefficient β , the temperature T and the
 192 pressure p :

$$V = V(V_0, \alpha, \beta, T, p) .$$

193 The volume relative uncertainty, $u(V)/V$, was estimated by using the standard formu-
 194 lation for the uncertainty propagation, as follows

$$\frac{u(V)}{V} = \frac{1}{V} \left[\left(\frac{\partial V}{\partial V_0} \right)^2 u^2(V_0) + \left(\frac{\partial V}{\partial \alpha} \right)^2 u^2(\alpha) + \left(\frac{\partial V}{\partial \beta} \right)^2 u^2(\beta) + \left(\frac{\partial V}{\partial T} \right)^2 u^2(T) + \left(\frac{\partial V}{\partial p} \right)^2 u^2(p) \right]^{\frac{1}{2}}, \quad (8)$$

195 where $u(V_0)$ is 0.002 cm^3 . The uncertainties of the α and β coefficients, $u(\alpha)$ and $u(\beta)$,
 196 are due to the fitting process for their estimations; other sources of uncertainty are neg-
 197 ligible.

198 The uncertainty on temperature, $u(T) = 0.01 \text{ K}$, was calculated by the uncertainty of
 199 the calibration fit, the instrument resolution, the reading repeatability and the tempera-
 200 ture gradient measured between the two thermometers. The uncertainty of the pressure
 201 transducer $u(p)$ is 0.01 MPa ; this value includes the declared uncertainty of the instru-
 202 ment at the full-scale and the repeatability.

203 In Table 1, all contributions to the relative uncertainty of the volume along with
 204 their relative values are reported.

205 3.4. Density uncertainty analysis

206 From the perspective of the uncertainty calculation, because seawater was measured
 207 by the pseudo-isochoric method, density is a function of mass, volume, and absolute
 208 salinity

$$\rho = \rho(m, V, S_A).$$

209 Applying the uncertainty propagation formula, the relative uncertainty of seawater den-
 210 sity is expressed by

$$\frac{u(\rho)}{\rho} = \frac{1}{\rho} \left[\left(\frac{\partial \rho}{\partial m} \right)^2 u^2(m) + \left(\frac{\partial \rho}{\partial V} \right)^2 u^2(V) + \left(\frac{\partial \rho}{\partial S_A} \right)^2 u^2(S_A) \right]^{\frac{1}{2}}, \quad (9)$$

211 where $u(m)$ is the mass uncertainty and is 0.002 g , while $u(V)$ is the uncertainty of the
 212 volume at the measured temperature and pressure, whose value is 0.003 cm^3 . Since
 213 the absolute salinity of the sample was not measured by the authors, its uncertainty,
 214 $u(S_A)$, was assumed starting from the value estimated by Le Menn (2011), combined
 215 with the value reported in McDougall et al. (2012). Table 1 summarizes all sources
 216 of uncertainty that play a role in the uncertainty budget of seawater density, and their
 217 relative magnitude.

218 The largest contribution to the uncertainty is due to the volume, as expected con-
 219 sidering the many quantities involved in its measurement. The expanded relative un-
 220 certainty of seawater density is 0.05% with a coverage factor $k = 2$, considering the
 221 worst case scenario.

Table 1: Uncertainty budget of standard seawater density ($S_A = 35.158 \text{ g}\cdot\text{kg}^{-1}$)

Uncertainty source	Relative magnitude %
Mass	0.015
Reading standard deviation	0.015
Balance resolution	0.001
Standard weights mass	negligible
Air density	negligible
Standard weights density	negligible
Volume	0.021
Reference volume	0.014
Mass of the reference fluid	0.013
Reference water density	0.003
Air density	negligible
Standard weights density	negligible
Temperature	0.001
Pressure	0.002
Thermal expansion coefficient	0.008
Compressibility coefficient	0.015
Temperature	0.001
Pressure	0.001
Salinity	<0.001
COMBINED UNCERTAINTY ($k = 2$)	0.05

222 4. Results

223 The density measurements were carried out for a sample of standard seawater deliv-
 224 ered by OSIL (Batch P160), with certified practical salinity $S_p = 34.993$, i.e., absolute
 225 salinity $S_A = 35.158 \text{ g}\cdot\text{kg}^{-1}$. Measurements were carried out at temperatures from
 226 about (261.15 to 313.15) K and in the pressure range between (21 to 110) MPa, for five
 227 samples of standard seawater of the same batch. All experimental densities along the
 228 constant-mass curves are listed in Table 2, where the values reported in italics identify
 229 metastable states.

230 Fig. 2 shows the pressure measurements as a function of temperature for each mea-
 231 suring cycle performed at constant mass. The measured thermodynamic states include
 232 also supercooled seawater region: the metastable equilibrium states. The plot of the
 233 densities as a function of temperature, along curves at constant mass, is reported in
 234 Fig. 3.

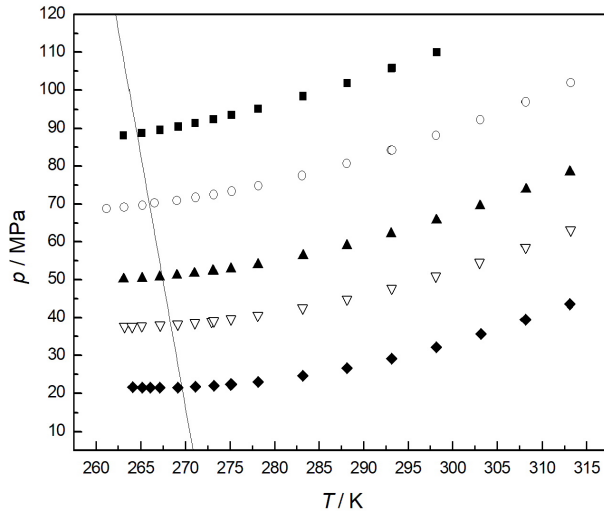


Figure 2: Pressure as a function of temperature at constant mass: \blacksquare , $m = 12.482$ g; \circ , $m = 12.371$ g; \blacktriangle , $m = 12.253$ g; ∇ , $m = 12.174$ g; \blacklozenge , $m = 12.069$ g; —, melting curve.

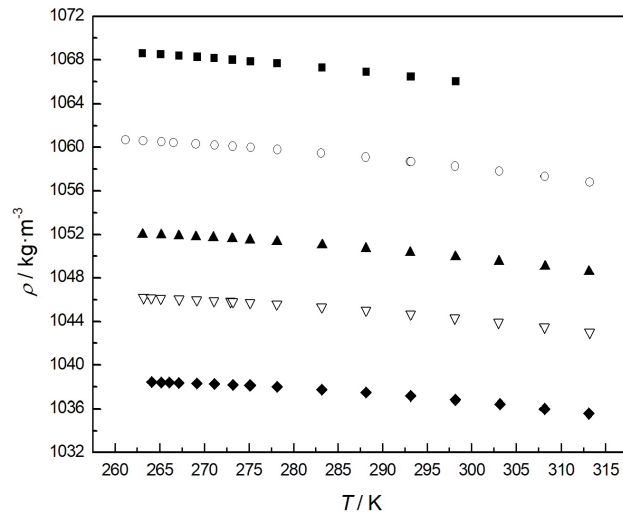


Figure 3: Density of standard seawater ($S_A = 35.158$ $\text{g}\cdot\text{kg}^{-1}$) as a function of temperature at constant mass: \blacksquare , $m = 12.482$ g; \circ , $m = 12.371$ g; \blacktriangle , $m = 12.253$ g; ∇ , $m = 12.174$ g; \blacklozenge , $m = 12.069$ g.

Table 2: Density ρ of standard seawater ($S_A = 35.158 \text{ g}\cdot\text{kg}^{-1}$) at temperature T and pressure p , for different masses m . The uncertainty associated with all values of density is 0.05 %. Entries in italics are the measurements carried out in metastable equilibrium.

T/K	p/MPa	$\rho/\text{kg}\cdot\text{m}^{-3}$	T/K	p/MPa	$\rho/\text{kg}\cdot\text{m}^{-3}$
$m = 12.482 \text{ g}$					
<i>263.10</i>	<i>88.10</i>	<i>1068.60</i>	275.18	93.55	1067.87
265.10	88.72	1068.50	278.18	95.16	1067.67
267.14	89.55	1068.39	283.20	98.43	1067.29
269.20	90.44	1068.26	288.17	101.82	1066.90
271.10	91.33	1068.15	293.13	105.71	1066.47
273.12	92.37	1068.02	293.21	105.84	1066.46
273.15	92.39	1068.01	298.23	109.96	1066.01
$m = 12.371 \text{ g}$					
<i>261.20</i>	<i>68.76</i>	<i>1060.68</i>	283.10	77.51	1059.46
<i>263.17</i>	<i>69.17</i>	<i>1060.60</i>	288.10	80.67	1059.09
<i>265.16</i>	<i>69.67</i>	<i>1060.52</i>	293.09	84.20	1058.70
266.55	70.26	1060.44	293.21	84.23	1058.69
269.05	70.94	1060.32	298.13	88.07	1058.27
271.15	71.73	1060.21	303.10	92.28	1057.82
273.17	72.47	1060.10	308.17	96.95	1057.33
275.20	73.36	1059.98	313.22	101.96	1056.81
278.18	74.79	1059.80			
$m = 12.253 \text{ g}$					
<i>263.10</i>	<i>50.17</i>	<i>1052.00</i>	278.15	54.00	1051.34
<i>265.15</i>	<i>50.37</i>	<i>1051.93</i>	283.21	56.37	1051.03
<i>267.13</i>	<i>50.71</i>	<i>1051.86</i>	288.16	59.02	1050.70
269.05	51.19	1051.77	293.10	62.14	1050.34
271.00	51.68	1051.69	298.20	65.73	1049.93
273.12	52.32	1051.59	303.09	69.52	1049.52
273.17	52.24	1051.59	308.21	73.90	1049.05
275.13	52.87	1051.50	313.14	78.48	1048.58
$m = 12.174 \text{ g}$					
<i>263.22</i>	<i>37.61</i>	<i>1046.18</i>	278.13	40.59	1045.59
<i>264.02</i>	<i>37.60</i>	<i>1046.16</i>	283.16	42.50	1045.32
<i>265.12</i>	<i>37.78</i>	<i>1046.12</i>	288.15	44.86	1045.02
<i>267.15</i>	<i>37.98</i>	<i>1046.06</i>	293.17	47.76	1044.67
269.14	38.25	1045.99	298.12	50.96	1044.30
271.07	38.62	1045.91	303.05	54.53	1043.91
272.95	38.94	1045.84	308.16	58.51	1043.48
273.20	39.11	1045.82	313.20	63.10	1043.00
275.14	39.61	1045.74			
$m = 12.069 \text{ g}$					
<i>264.10</i>	<i>21.57</i>	<i>1038.44</i>	278.15	23.05	1037.99
<i>265.16</i>	<i>21.54</i>	<i>1038.42</i>	283.18	24.64	1037.75

(Continued on next page)

(Continued from previous page)

266.05	21.54	1038.39	288.15	26.67	1037.48
267.14	21.53	1038.37	293.15	29.17	1037.16
269.15	21.54	1038.32	298.16	32.13	1036.82
271.13	21.71	1038.26	303.17	35.70	1036.42
273.21	21.98	1038.19	308.14	39.46	1036.01
275.05	22.34	1038.12	313.11	43.54	1035.58
275.16	22.34	1038.12			

235 The experimental densities of this work were compared to the density values pro-
236 vided by TEOS-10 formulation. Figs. 4 and 5 show the deviations of the measurements
237 from TEOS-10 equation as a function of temperature and pressure, respectively. All the
238 deviations are within $\pm 0.02\%$, so considering the experimental uncertainty all measure-
239 ments are in good agreement with TEOS-10. From Fig. 4, it is possible to note that most
240 of the largest deviations correspond to the lowest temperature, and in particular to mes-
241 tatable states. Also observing Fig. 5, it is clear that the largest deviations correspond
242 to the lowest pressures, thus measurements carried out in the metastable region.

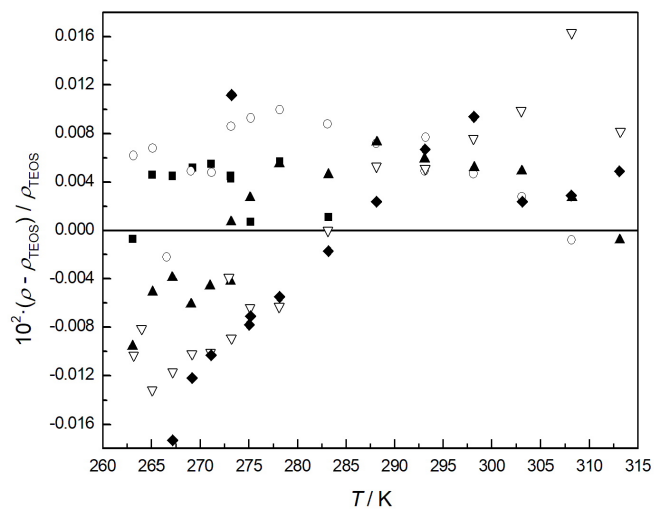


Figure 4: Deviations of experimental seawater density from the values of TEOS-10 (zero line) as a function of temperature: ■, $m = 12.482$ g; ○, $m = 12.371$ g; ▲, $m = 12.253$ g; ▽, $m = 12.174$ g; ◆, $m = 12.069$ g.

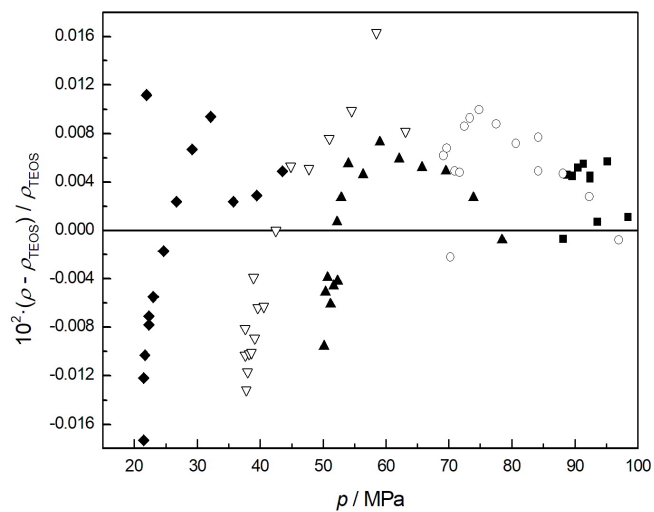


Figure 5: Deviations of experimental seawater density from the values of TEOS-10 (zero line) as a function of pressure: ■, $m = 12.482$ g; ○, $m = 12.371$ g; ▲, $m = 12.253$ g; ▽, $m = 12.174$ g; ◆, $m = 12.069$ g.

Table 3: Coefficients for the interpolation function of density (Eq. 10) determined from the experimental densities, temperatures and pressures by means of the least squares method.

parameter	value	unit
a	0.182915	$\text{m}^3 \cdot \text{kg}^{-1} \cdot \text{MPa}$
b	$6.97805 \cdot 10^{-4}$	$\text{m}^3 \cdot \text{kg}^{-1}$
c	659.033	MPa
t_a	$-4.66555 \cdot 10^{-5}$	K^{-2}
t_b	8.82548	K^{-1}
t_c	$1.40672 \cdot 10^{-3}$	K^{-1}
t_d	$-6.07869 \cdot 10^{-5}$	K^{-2}
t_e	$-5.93252 \cdot 10^{-8}$	K^{-3}

243 5. Derived thermal properties

244 The measurements presented in this work, together with the experimental results of
 245 Romeo et al. (2019), carried out by means of a commercial vibrating tube densimeter
 246 at atmospheric pressure, were regressed to identify a model to calculate density. The
 247 model was chosen to be slender and handy, trying to balance the need for a very limited
 248 number of parameters and good accuracy. The model used is the following 8-parameters
 249 equation:

$$v(T, p) = \frac{a[1 + t_a(T - T_0)^2]}{p + c[1 + t_c(T - T_0) + t_d(T - T_0)^2 + t_e(T - T_0)^3]} + b[1 + t_b(T - T_0)], \quad (10)$$

250 where $v(T, p)$ is the specific volume and $a, b, c, t_a, t_b, t_c, t_d, t_e$ are parameters, whose
 251 values are shown in Tab. 3. Validity of Eq 10 was checked analyzing the residuals
 252 of the fit. In Figs. 6 and 7, relative difference between fit-predicted and experimental
 253 densities as a function of temperature and pressure, respectively, are shown. Residuals
 254 spread within $\pm 0.012\%$ and most of them within $\pm 0.007\%$, so widely less than the
 255 experimental uncertainty.

256 Equation 10 was used to calculate seawater density, isothermal compressibility and
 257 isobaric thermal expansion, in the temperature range between (263.15 to 313.15) K,
 258 with step of 10 K, and in the pressure range between (1 to 105) MPa. The set of den-
 259 sity, isothermal compressibility and thermal expansivity data is reported in Tab. 4.
 260 Fig. 8 shows the densities obtained by Eq. 10 as a function of pressure along isotherms.
 261 Comparison between the calculated densities and TEOS-10 values is reported in Fig. 9.
 262 The deviations scatter within $\pm 0.015\%$. Based on these results, Eq. 10 can be used to
 263 calculate density within the fitted $T - p$ range with the same uncertainty value stated
 264 for the experimental density, i.e., 0.05 %.

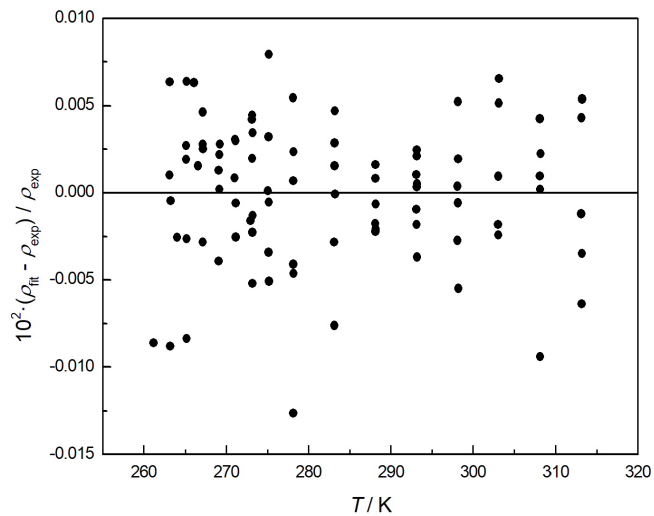


Figure 6: Percentage residuals of the fit (predicted density versus experimental density) as a function of temperature.

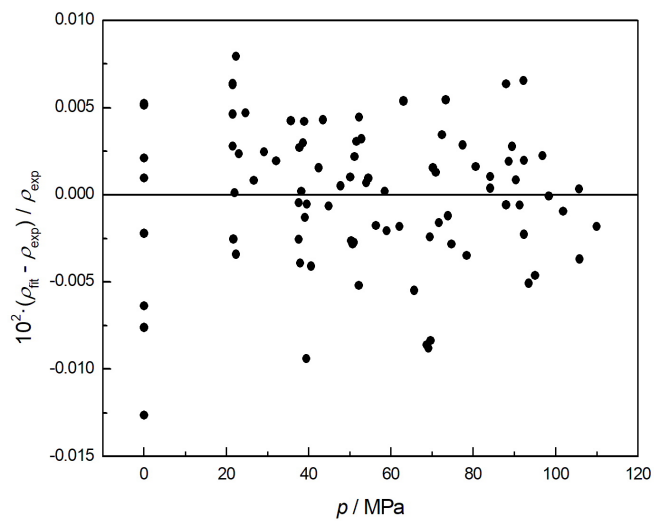


Figure 7: Percentage residuals of the fit (predicted density versus experimental density) as a function of pressure.

Table 4: Density ρ of standard seawater ($S_A = 35.158 \text{ g}\cdot\text{kg}^{-1}$) at temperature T and pressure p , calculated by using Eq.10 along with the isothermal compressibility κ and the isobaric thermal expansion α . Entries in italics refer to metastable states of liquid seawater.

p / MPa	$\rho / \text{kg}\cdot\text{m}^{-3}$	κ / GPa^{-1}	$10^4 \cdot \alpha / \text{K}^{-1}$
$T = 263.15 \text{ K}$			
<i>1.00</i>	<i>1028.23</i>	<i>0.4969</i>	<i>-0.818</i>
<i>15.00</i>	<i>1035.27</i>	<i>0.4779</i>	<i>-0.321</i>
<i>30.00</i>	<i>1042.57</i>	<i>0.4587</i>	<i>0.178</i>
<i>45.00</i>	<i>1049.62</i>	<i>0.4407</i>	<i>0.645</i>
<i>60.00</i>	<i>1056.45</i>	<i>0.4237</i>	<i>1.083</i>
<i>75.00</i>	<i>1063.06</i>	<i>0.4077</i>	<i>1.493</i>
<i>90.00</i>	<i>1069.46</i>	<i>0.3926</i>	<i>1.879</i>
<i>105.00</i>	<i>1075.66</i>	<i>0.3926</i>	<i>2.241</i>
$T = 273.15 \text{ K}$			
1.00	1028.37	0.4655	0.500
15.00	1034.97	0.4484	0.861
30.00	1041.82	0.4310	1.226
45.00	1048.45	0.4147	1.568
60.00	1054.87	0.3993	1.891
75.00	1061.09	0.3848	2.195
90.00	1067.12	0.3710	2.481
105.00	1072.66	0.3580	2.752
$T = 283.15 \text{ K}$			
1.00	1027.29	0.4431	1.581
15.00	1033.56	0.4272	1.834
30.00	1040.08	0.4111	2.090
45.00	1046.39	0.3959	2.332
60.00	1052.51	0.3816	2.560
75.00	1058.44	0.3680	2.777
90.00	1064.20	0.3551	2.982
105.00	1069.78	0.3429	3.177
$T = 293.15 \text{ K}$			
1.00	1025.17	0.4280	2.517
15.00	1031.23	0.4129	2.677
30.00	1037.51	0.3976	2.840
45.00	1043.60	0.3831	2.995
60.00	1049.51	0.3694	3.143
75.00	1055.24	0.3564	3.284
90.00	1060.79	0.3441	3.419
105.00	1066.19	0.3324	3.548
$T = 303.15 \text{ K}$			
1.00	1022.15	0.4195	3.376
15.00	1028.07	0.4047	3.451

(Continued on next page)

(Continued from previous page)

30.00	1034.21	0.3897	3.528
45.00	1040.16	0.3756	3.604
60.00	1045.93	0.3622	3.677
75.00	1051.53	0.3495	3.749
90.00	1056.96	0.3374	3.818
105.00	1062.23	0.3260	3.886
$T = 313.15 \text{ K}$			
1.00	1018.28	0.4172	4.219
15.00	1024.14	0.4023	4.209
30.00	1030.22	0.3873	4.202
45.00	1036.11	0.3731	4.198
60.00	1041.82	0.3597	4.198
75.00	1047.36	0.3470	4.200
90.00	1052.73	0.3350	4.205
105.00	1057.94	0.3235	4.212

265 In Fig. 10 the derived isothermal compressibility as a function of pressure, along
266 isotherms is shown. Compressibility results are compared to TEOS-10 values and
267 shown in Fig. 11. Difference of isothermal compressibility are lower than 0.005 GPa^{-1}
268 and, as expected, are higher for the isotherm of supercooled seawater. This latter is
269 also the only isotherm for which the differences have an opposite trend compared to
270 the others. Calculated isobaric thermal expansion as a function of pressure and repre-
271 sented along isotherms are reported in Fig. 12. Whereas in Fig. 13, expansivities of
272 this work and TEOS-10 are compared. Differences are lower than $0.24 \cdot 10^{-4} \text{ K}^{-1}$, and
273 the two isotherms at the extreme temperatures show the highest differences, which are
274 at the lowest pressure. Instead, for the intermediate temperatures, the differences are
275 nearly constant.

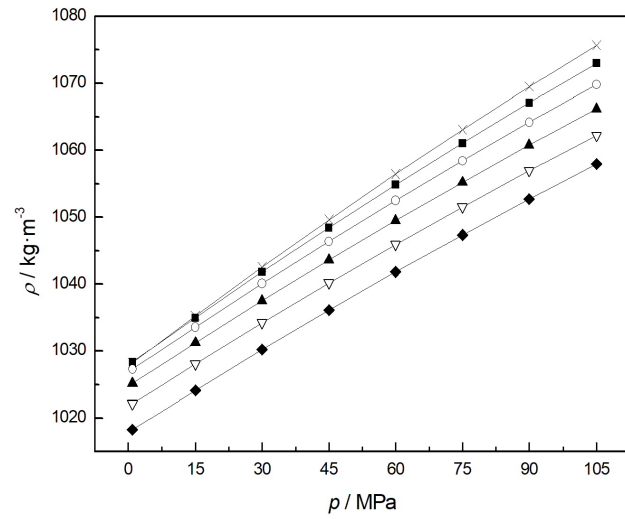


Figure 8: Density of seawater calculated by the fit (Eq. 10) as a function pressure, along isotherms: \times , $T = 263.15$ K; \blacksquare , $T = 273.15$ K; \circ , $T = 283.15$ K; \blacktriangle , $T = 293.15$ K; ∇ , $T = 303.15$ K; \blacklozenge , $T = 313.15$ K.

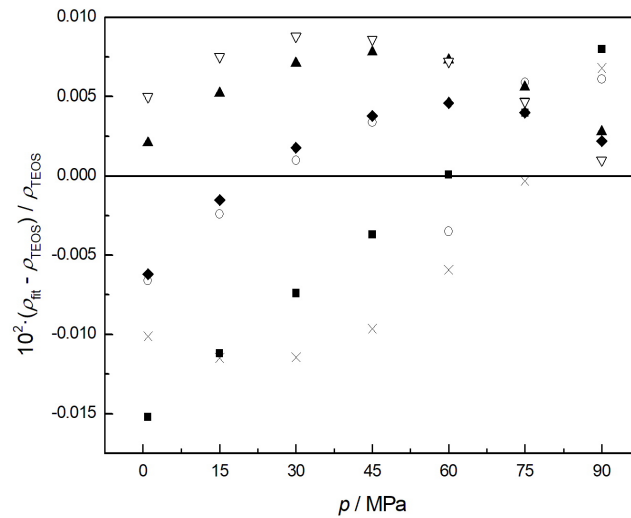


Figure 9: Percentage deviations of seawater densities calculated by the fit (Eq. 10) from the values of TEOS-10 (zero line) as a function pressure, along isotherms: \times , $T = 263.15$ K; \blacksquare , $T = 273.15$ K; \circ , $T = 283.15$ K; \blacktriangle , $T = 293.15$ K; ∇ , $T = 303.15$ K; \blacklozenge , $T = 313.15$ K.

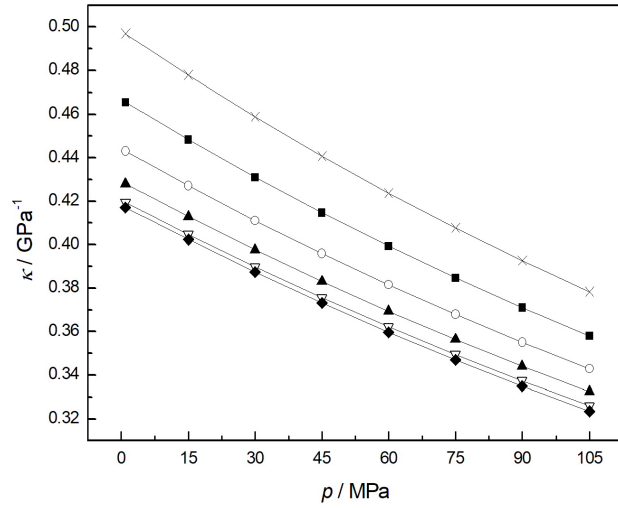


Figure 10: Isothermal compressibility of seawater as a function of pressure: \times , $T = 263.15$ K; \blacksquare , $T = 273.15$ K; \circ , $T = 283.15$ K; \blacktriangle , $T = 293.15$ K; ∇ , $T = 303.15$ K; \blacklozenge , $T = 313.15$ K.

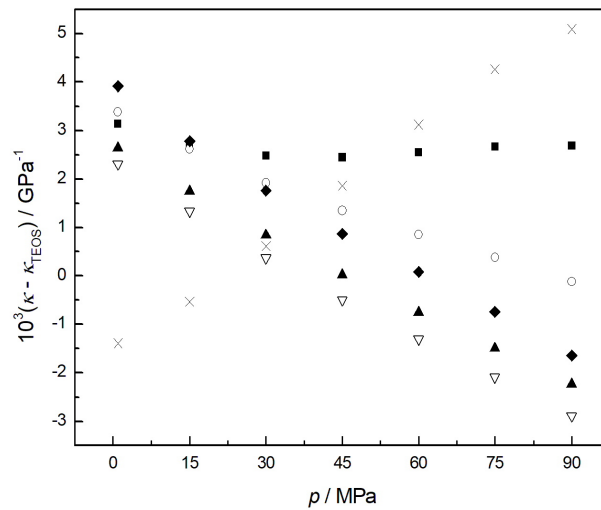


Figure 11: Deviations of isothermal compressibility derived in this work from data calculated by TEOS-10 as a function of pressure: \times , $T = 263.15$ K; \blacksquare , $T = 273.15$ K; \circ , $T = 283.15$ K; \blacktriangle , $T = 293.15$ K; ∇ , $T = 303.15$ K; \blacklozenge , $T = 313.15$ K.

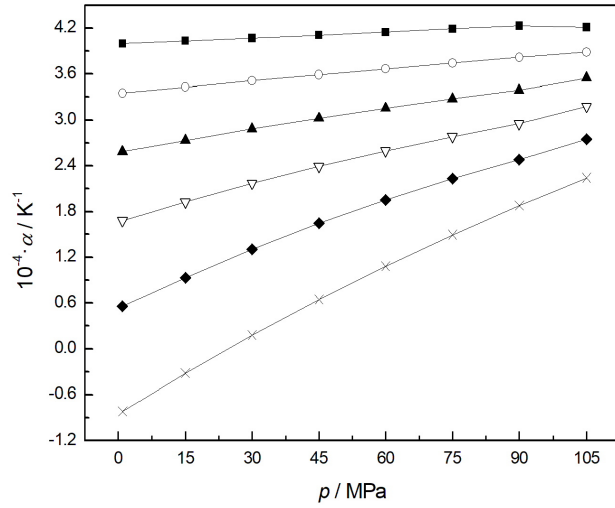


Figure 12: Isobaric thermal expansion of seawater as a function of pressure: \times , $T = 263.15$ K; \blacksquare , $T = 273.15$ K; \circ , $T = 283.15$ K; \blacktriangle , $T = 293.15$ K; ∇ , $T = 303.15$ K; \blacklozenge , $T = 313.15$ K.

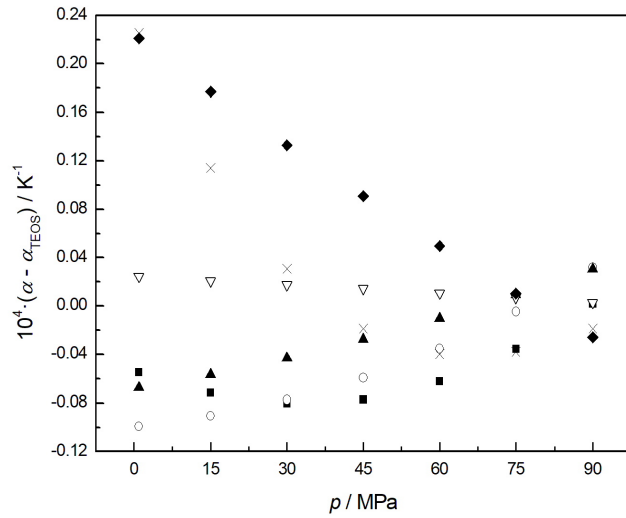


Figure 13: Deviations of isobaric thermal expansion derived in this work from data calculated by TEOS-10 as a function of pressure: \times , $T = 263.15$ K; \blacksquare , $T = 273.15$ K; \circ , $T = 283.15$ K; \blacktriangle , $T = 293.15$ K; ∇ , $T = 303.15$ K; \blacklozenge , $T = 313.15$ K.

276 **6. Conclusions**

277 In this work, with the pseudo-isochoric method, density of standard seawater ($S_A =$
278 $35.158 \text{ g}\cdot\text{kg}^{-1}$) was measured. Measurements were carried out by means of a calibrated
279 pycnometer of known volume as a function of temperature and pressure. The mass of
280 seawater was determined by the gravimetric method. Seawater density was obtained for
281 temperatures between (261.15 to 313.15) K and in the pressure range from about (21 to
282 110) MPa, thus partially covering the supercooled region, with an estimated expanded
283 relative uncertainty of 0.05 %, with $k = 2$. The experimental values were compared
284 to the equation of state of TEOS-10 (IOC et al., 2010). Considering the experimental
285 uncertainty, all the measurements are in agreement with TEOS-10 data within ± 0.02 %.

286 Starting from the high pressure experimental data, along with the measurements at
287 atmospheric pressure of Romeo et al. (2019), a 8-parameters function of specific vol-
288 ume as a function of temperature and pressure was implemented. The function is able to
289 determine seawater density from (263.15 to 313.15) K and from (1 to 105) MPa, with
290 an uncertainty of 0.05 %. Additionally, from the calculated densities, the isothermal
291 compressibilities and the isobaric thermal expansivities were derived and compared
292 with the values of TEOS-10, resulting within $\pm 0.005 \text{ GPa}^{-1}$ and $\pm 0.24 \cdot 10^{-4} \text{ K}^{-1}$, re-
293 spectively.

294 **Acknowledgements**

295 The authors would like to thank the International Association for Properties of Water
296 and Steam for the collaboration and for giving suggestions and ideas for this and future
297 works.

298 **References**

- 299 BIPM, IEC, IFCC, ILAC, ISO, IUPAC, IUPAP, OILM, 2008. Evaluation of measure-
300 ment data – Guide to the expression of uncertainty in measurements, JMGM 100:
301 2008 GUM 1995 with minor corrections.
- 302 Davidson, S., Perkin, M., Buckley, M., 2004. The measurement of mass and weight.
303 National Physical Laboratory.
- 304 Feistel, R., 2018. Thermodynamic properties of seawater, ice and humid air: TEOS-10,
305 before and beyond. *Ocean Sci.* 14, 471-502.
- 306 Goodwin, A.R.H., Marsh, W.A., Wakeham, W.A., 2003. Measurement of the Thermo-
307 dynamic Properties of Single Phases, *Experimental Thermodynamics*. Elsevier, Vol.
308 VI.
- 309 Haumann, F.A., Moorman, R., Riser, S., Smedsrud, L.H., Maksym, T., Wong, A.P.S.,
310 Wilson, E.A., Drucker, R., Talley, L.D., Johnson, K.S., Key, R.M., Sarmiento, J.L.
311 2020, *Geophys. Res. Lett.* 47, e2020GL090242.

- 312 Hoppmann, M., Richter, M.E., Smith, I.J., Jendersie, S., Langhorne, P.J., Thomas, D.N.,
313 Dieckmann, G.S., 2020. 1 (2020). Platelet ice, the Southern Ocean's hidden ice: a
314 review. *Ann. Glaciol.*, 1-28.
- 315 IOC, SCOR, IAPSO, 2010. The international thermodynamic equation of seawater –
316 2010: Calculation and use of thermodynamic properties. Intergovernmental oceanographic
317 Commission, Manuals and Guides n. 56, UNESCO (English), 196.
- 318 Katlein, C., Mohrholz, V., Sheikin, I., Itkin, P., Divine, D.V., Stroeve, J., et al. 2020.
319 *Geophys. Res. Lett.* 47, e2020GL088898 (2020).
- 320 Le Menn, M., 2011. About uncertainties in practical salinity calculations. *Ocean Sci.*
321 7, 651–659.
- 322 Loreface, S., Romeo, R., Santiano, M., Capelli, A., 2014. Original pycnometers for
323 volatile liquid density over wide ranges of temperature and pressure: practical example.
324 *Metrologia* 51, 154-160.
- 325 McDougall, T.J., Jackett, D.R., Millero, F.J., Pawlowicz, R., Baker, P.M., 2012. A
326 global algorithm for estimating Absolute Salinity. *Ocean Sci.* 8, 1123-1134.
- 327 OIML R111-1 (E), 2004. Weights of Classes E₁, E₂, F₁, F₂, M₁, M₁₋₂, M₂₋₃ and M₃,
328 Part 1: Metrological and technical requirements, International Organization of Legal
329 Metrology.
- 330 Romeo, R., Giuliano Albo, P.A., Lago, S., 2019. Density of standard seawater by vibrating
331 tube densimeter: Analysis of the method and results. *Deep-Sea Res. I* 154,
332 103157.
- 333 Romeo, R., Lago, S., Giuliano Albo, P.A., 2018. Experimental densities of subcooled
334 deuterium oxide at pressures up to 160 MPa. *J. Chem. Phys.* 149, 154503.
- 335 Safarov, J., Berndt, S., Millero, F., Feistel, R., Heintz, A., Hassel, E., 2012. (p, ρ, T)
336 properties of seawater: Extensions to high salinities. *Deep-Sea Res. I* 65, 146-156.
- 337 Safarov, J., Berndt, S., Millero, F.J., Feistel, R., Heintz, A., Hassel, E.P., 2013. (p, ρ, T)
338 Properties of seawater at brackish salinities: Extensions to high temperatures and
339 pressures. *Deep-Sea Res. I* 78, 95-101.
- 340 Safarov, J., Millero, F., Feistel, R., Heintz, A., Hassel, E., 2009. Thermodynamic properties
341 of standard seawater: extensions to high temperatures and pressure. *Ocean Sci.*
342 5, 235-246.
- 343 Seitz, S., Feistel, R., Wright, D.G., Weinreben, S., Spitzer, P., De Bièvre, P., 2011.
344 Metrological traceability of oceanographic salinity measurement results. *Ocean Sci.*
345 7, 45-62.
- 346 Wagner, W., Pruss, A., 2002. The IAPWS formulation 1995 for the thermodynamic
347 properties of ordinary water substance for general and scientific use. *J. Phys. Chem.*
348 *Ref. Data* 31, 387-535.

349 Wright, D.G., Pawlowicz, R., McDougall, T.J., Feistel, R., Marion, G.M., 2011. Ab-
350 solute Salinity, “Density Salinity” and the Reference-Composition Salinity Scale:
351 present and future use in the seawater standard TEOS-10. *Ocean Sci.* 7, 1-26.